

Plasmon excitations in layered high- T_c cuprates

Andrés Greco[†], Hiroyuki Yamase[‡], and Matías Bejas[†]

[†]*Facultad de Ciencias Exactas, Ingeniería y Agrimensura
and Instituto de Física Rosario (UNR-CONICET),
Av. Pellegrini 250, 2000 Rosario, Argentina*

[‡]*National Institute for Materials Science, Tsukuba 305-0047, Japan*

(Dated: November 25, 2021)

Abstract

Motivated by the recent resonant inelastic x-ray scattering (RIXS) experiment for the electron-doped cuprates $\text{Nd}_{2-x}\text{Ce}_x\text{CuO}_4$ with $x \approx 0.15$, we compute the density-density correlation function in the t - J model on a square lattice by including interlayer hopping and the long-range Coulomb interaction. We find that collective charge excitations are realized not inside the particle-hole continuum, but above the continuum as plasmons. The plasmon mode has a rather flat dispersion near the in-plane momentum $\mathbf{q}_{\parallel} = (0, 0)$ with a typical excitation energy of the order of the intralayer hopping t when the out-of-plane momentum q_z is zero. However, when q_z becomes finite, the plasmon dispersion changes drastically near $\mathbf{q}_{\parallel} = (0, 0)$, leading to a strong dispersive feature with an excitation gap scaled by the interlayer hopping t_z . We discuss the mode recently observed by RIXS near $\mathbf{q}_{\parallel} = (0, 0)$ in terms of the plasmon mode with a finite q_z .

PACS numbers: 75.25.Dk, 78.70.Ck, 74.72.-h

I. INTRODUCTION

Recently x-ray scattering revealed charge excitations for various hole-doped cuprates such as Y-¹⁻⁵, Bi-⁶⁻⁸, and Hg-based⁹ compounds, which attracts renewed interest. An intriguing aspect is that the charge excitations are not closely connected with spin excitations, in contrast to the well-known case of La-based cuprates, where spin-charge stripes were discussed¹⁰. Another intriguing aspect is that the charge-excitation signals develop inside the pseudogap state, whose origin is still a controversial issue in high-temperature cuprate superconductors.

As in the hole-doped cuprates, charge excitations were also observed in electron-doped cuprates $\text{Nd}_{2-x}\text{Ce}_x\text{CuO}_4$ (NCCO) with $x \approx 0.15$ (Ref. 11). The situation in the electron-doped cuprates seems transparent in the sense that the pseudogap is not detected in a superconducting sample above its onset temperature (T_c) (Ref. 12). Thus, the state above T_c can be approximated as a normal metallic state. In fact, the charge excitations observed by resonant x-ray scattering (RXS)¹¹ are well captured by assuming a paramagnetic state in the t - J model¹³. Ref. 13 shows that the observed charge excitations can be associated with a d -wave bond order and its low-energy collective excitations are realized around $\mathbf{q} = (0.49\pi, 0)$ and $(0.84\pi, 0.84\pi)$; the former agrees with the RXS results¹¹ and the latter is a theoretical prediction. There are also individual charge excitations associated with the d -wave bond order, emerging from $\mathbf{q} = (0, 0)$ and $\omega = 0$. These excitations are dominant at a relatively low energy scale of $\sim 0.1t$ where t is a bare hopping integral in the model.

What kind of charge excitations can then occur at a relatively high energy in the normal metallic phase? In particular, recent resonant inelastic x-ray scattering (RIXS) for NCCO reveals a dispersive signal, which has a typical energy of 0.3 eV around $\mathbf{q} = (0, 0)$ and increases to 1 eV around $\mathbf{q} = (0.3\pi, 0)$ ^{14,15}. While it is not fully clear at the moment that those excitations can be understood also in terms of bond-order charge excitations¹³, one alternative possibility is plasmon excitations, whose energy is typically around 1 eV in cuprates as observed in optical measurements¹⁶ and electron energy-loss spectroscopy (EELS)^{17,18}. In addition, the plasmon itself is a general phenomenon in an electronic system and is described by the usual on-site density-density response function, i.e., the dielectric function. Hence we expect generally that plasmon excitations become relevant to the charge dynamics especially in a high energy region.

In the context of cuprates, plasmons were considered as a mechanism to enhance the

onset temperature of superconductivity in the presence of electron-phonon coupling^{19,20} and were also studied across the metal-insulator transition²¹. In particular, it was argued theoretically²² that the plasmon can be detected by RIXS.

In this paper, we study plasmon excitations in the normal metallic phase by including the long-range Coulomb interaction V , which is crucially important to plasmons. We also include interlayer hopping as a generic model for cuprate superconductors and study the t - J - V model on a layered square-lattice. We invoke a large- N scheme formulated in the framework of the t - J model²³, which successfully captures the recent RIXS data for NCCO¹³. We find that when q_z (out-of-plane momentum transfer) is zero, the plasmon mode has a gap at $\mathbf{q}_{\parallel} = (0, 0)$ and exhibits a weak dispersive feature away from $\mathbf{q}_{\parallel} = (0, 0)$; here \mathbf{q}_{\parallel} denotes in-plane momentum transfer. At finite q_z , however, the plasmon energy decreases substantially at $\mathbf{q}_{\parallel} = (0, 0)$, but still retains a gap. This gap magnitude is scaled by the interlayer hopping amplitude t_z . Away from $\mathbf{q}_{\parallel} = (0, 0)$ the plasmon exhibits a dispersion similar to the experimental observation in electron-doped cuprates¹⁵. Our obtained results are expected to be general for layered cuprates, implying a similar plasmon mode also in hole-doped cuprates, which can be tested by RIXS.

Our theoretical study shares the importance of plasmons to the RIXS spectrum with Ref. 22. The differences from the previous work²² are in the inclusion of t_z , a functional form of the long-range Coulomb interaction, and a strong-coupling theory formulated in the t - J model. These differences, mainly the former two, yield charge excitation spectra different from Ref. 22.

In Sec. II we describe the model and formalism. Our results are presented in Sec. III and discussed in Sec. IV. Conclusions are given in Sec. V.

II. MODEL AND FORMALISM

Cuprate superconductors are layered materials where the conducting electrons are confined to the CuO_2 planes, which are weakly coupled to each other along the z direction. In order to address the recently observed charge excitations near $\mathbf{q}_{\parallel} = (0, 0)$ ^{14,15}, we study the t - J model on a square lattice by including both interlayer hopping and the long-range

Coulomb interaction, namely a layered t - J - V model:

$$H = - \sum_{i,j,\sigma} t_{ij} \tilde{c}_{i\sigma}^\dagger \tilde{c}_{j\sigma} + \sum_{\langle i,j \rangle} J_{ij} \left(\vec{S}_i \cdot \vec{S}_j - \frac{1}{4} n_i n_j \right) + \frac{1}{2} \sum_{i,j} V_{ij} n_i n_j \quad (1)$$

where the sites i and j run over a three-dimensional lattice. The hopping t_{ij} takes a value t (t') between the first (second) nearest-neighbors sites on the square lattice whereas hopping integrals between the layers are scaled by t_z and we will specify the out-of-plane dispersion later [see Eq. (9)]. $\langle i, j \rangle$ indicates a nearest-neighbor pair of sites on the square lattice, and we consider the exchange interaction only inside the plane, namely $J_{ij} = J$ because the exchange term between adjacent planes is much smaller than J (Ref. 24). V_{ij} is the long-range Coulomb interaction on the lattice and is given in momentum space by

$$V(\mathbf{q}) = \frac{V_c}{A(q_x, q_y) - \cos q_z}, \quad (2)$$

where $V_c = e^2 d (2\epsilon_\perp a^2)^{-1}$ and

$$A(q_x, q_y) = \frac{\tilde{\epsilon}}{(a/d)^2} (2 - \cos q_x - \cos q_y) + 1. \quad (3)$$

These expressions are easily obtained by solving Poisson's equation on a lattice²⁵. Here $\tilde{\epsilon} = \epsilon_\parallel / \epsilon_\perp$, and ϵ_\parallel and ϵ_\perp are the dielectric constants parallel and perpendicular to the planes, respectively, and they are positive; $V(\mathbf{q})$ is thus positive for any \mathbf{q} ; a and d are the lattice spacing in the planes and between the planes, respectively; e is the electric charge of electrons. In the present study, momentum is measured in units of the inverse of the lattice constants in each direction, namely a^{-1} along the x and y direction and d^{-1} along the z direction. $\tilde{c}_{i\sigma}^\dagger$ ($\tilde{c}_{i\sigma}$) is the creation (annihilation) operator of electrons with spin σ ($\sigma = \downarrow, \uparrow$) in the Fock space without double occupancy. $n_i = \sum_\sigma \tilde{c}_{i\sigma}^\dagger \tilde{c}_{i\sigma}$ is the electron density operator and \vec{S}_i is the spin operator.

We analyze the model (1) in terms of a large- N expansion formulated in Ref. 23 for Hubbard operators. While it was formulated for the purely two-dimensional t - J model, it is straightforward to extend it to the present layered model. Since the method was described in previous papers^{23,26,27}, here we reproduce only the main details. In the large- N scheme, the charge excitations are described by a six-component bosonic field, namely δX^a with $a = 1, 2, \dots, 6$. δX^1 describes on-site charge fluctuations and δX^2 fluctuations around the mean value of a Lagrange multiplier associated with the constraint of non-double occupancy. δX^3 and δX^4 (δX^5 and δX^6) describe real (imaginary) parts of bond-field fluctuations along

the x and y directions, respectively; the expectation value of the bond field is specified later [Eq. (10)]. The six-component boson propagator is then given by a 6×6 matrix. At leading order, the inverse of the propagator is given by

$$D_{ab}^{-1}(\mathbf{q}, i\omega_n) = [D_{ab}^{(0)}(\mathbf{q}, i\omega_n)]^{-1} - \Pi_{ab}(\mathbf{q}, i\omega_n). \quad (4)$$

Here a and b run from 1 to 6, ω_n is a bosonic Matsubara frequency, and $D_{ab}^{(0)}(\mathbf{q}, i\omega_n)$ is a bare bosonic propagator

$$[D_{ab}^{(0)}(\mathbf{q}, i\omega_n)]^{-1} = N \begin{pmatrix} \frac{\delta^2}{2} (V(\mathbf{q}) - J(\mathbf{q})) & \frac{\delta}{2} & 0 & 0 & 0 & 0 \\ \frac{\delta}{2} & 0 & 0 & 0 & 0 & 0 \\ 0 & 0 & \frac{4\Delta^2}{J} & 0 & 0 & 0 \\ 0 & 0 & 0 & \frac{4\Delta^2}{J} & 0 & 0 \\ 0 & 0 & 0 & 0 & \frac{4\Delta^2}{J} & 0 \\ 0 & 0 & 0 & 0 & 0 & \frac{4\Delta^2}{J} \end{pmatrix}, \quad (5)$$

with $J(\mathbf{q}) = \frac{J}{2}(\cos q_x + \cos q_y)$. $\Pi_{ab}(\mathbf{q}, i\omega_n)$ are the bosonic self-energies at leading order:

$$\begin{aligned} \Pi_{ab}(\mathbf{q}, i\omega_n) = & -\frac{N}{N_s N_z} \sum_{\mathbf{k}} h_a(\mathbf{k}, \mathbf{q}, \varepsilon_{\mathbf{k}} - \varepsilon_{\mathbf{k}-\mathbf{q}}) \frac{n_F(\varepsilon_{\mathbf{k}-\mathbf{q}}) - n_F(\varepsilon_{\mathbf{k}})}{i\omega_n - \varepsilon_{\mathbf{k}} + \varepsilon_{\mathbf{k}-\mathbf{q}}} h_b(\mathbf{k}, \mathbf{q}, \varepsilon_{\mathbf{k}} - \varepsilon_{\mathbf{k}-\mathbf{q}}) \\ & -\delta_{a1} \delta_{b1} \frac{N}{N_s N_z} \sum_{\mathbf{k}} \frac{\varepsilon_{\mathbf{k}} - \varepsilon_{\mathbf{k}-\mathbf{q}}}{2} n_F(\varepsilon_{\mathbf{k}}). \end{aligned} \quad (6)$$

The factor N in front of Eqs. (5) and (6) comes from the sum over the N fermionic channels after the extension of the spin index σ from 2 to N , whereas N_s and N_z are the total number of lattice sites on the square lattice and the number of layers along the z direction, respectively. The electronic dispersion $\varepsilon_{\mathbf{k}}$ may be written as

$$\varepsilon_{\mathbf{k}} = \varepsilon_{\mathbf{k}}^{\parallel} + \varepsilon_{\mathbf{k}}^{\perp} \quad (7)$$

where the in-plane dispersion $\varepsilon_{\mathbf{k}}^{\parallel}$ and the out-of-plane dispersion $\varepsilon_{\mathbf{k}}^{\perp}$ are given by, respectively,

$$\varepsilon_{\mathbf{k}}^{\parallel} = -2 \left(t \frac{\delta}{2} + \Delta \right) (\cos k_x + \cos k_y) - 4t' \frac{\delta}{2} \cos k_x \cos k_y - \mu, \quad (8)$$

$$\varepsilon_{\mathbf{k}}^{\perp} = 2t_z \frac{\delta}{2} (\cos k_x - \cos k_y)^2 \cos k_z. \quad (9)$$

The functional form $(\cos k_x - \cos k_y)^2$ in $\varepsilon_{\mathbf{k}}^{\perp}$ is frequently invoked for cuprates²⁸. Here δ is doping rate, μ the chemical potential, and Δ the mean-field value of the bond-field. For a

given δ , μ and Δ are determined self-consistently by solving

$$\Delta = \frac{J}{4N_s N_z} \sum_{\mathbf{k}} (\cos k_x + \cos k_y) n_F(\varepsilon_{\mathbf{k}}), \quad (10)$$

$$(1 - \delta) = \frac{2}{N_s N_z} \sum_{\mathbf{k}} n_F(\varepsilon_{\mathbf{k}}), \quad (11)$$

where n_F is the Fermi function. The six-component vertex h_a in Eq. (6) is given by

$$h_a(\mathbf{k}, \mathbf{q}, \nu) = \left\{ \begin{aligned} & \frac{2\varepsilon_{\mathbf{k}-\mathbf{q}} + \nu + 2\mu}{2} + 2\Delta \left[\cos\left(k_x - \frac{q_x}{2}\right) \cos\left(\frac{q_x}{2}\right) + \cos\left(k_y - \frac{q_y}{2}\right) \cos\left(\frac{q_y}{2}\right) \right]; 1; \\ & -2\Delta \cos\left(k_x - \frac{q_x}{2}\right); -2\Delta \cos\left(k_y - \frac{q_y}{2}\right); 2\Delta \sin\left(k_x - \frac{q_x}{2}\right); 2\Delta \sin\left(k_y - \frac{q_y}{2}\right) \end{aligned} \right\}. \quad (12)$$

We compute the on-site density-density correlation function in the present large- N framework. After summing all contributions up to $O(1/N)$, we obtain

$$\chi^c(\mathbf{q}, i\omega_n) = -N \left(\frac{\delta}{2}\right)^2 D_{11}(\mathbf{q}, i\omega_n). \quad (13)$$

Thus, the density-density correlation function is connected with the component (1, 1) of the D_{ab} .

Although the physical value is $N = 2$, the large- N expansion has several advantages over usual perturbations theories. First, in contrast to usual random-phase approximation (RPA) which is valid in the weak coupling regime, χ^c is not obtained as perturbation of any physical parameters of the model (1). This difference is crucial near half-filling where strong correlations are expected to be important. In fact, charge degrees of freedom are generated by carrier doping into a Mott insulator and thus the long-range part of the Coulomb interaction should vanish at half-filling. This feature is captured already in the present leading order theory [see the (1, 1) component in Eq. (5)], but not in weak coupling²⁹. Second, it was shown³⁰ that the large- N expansion reproduces well charge excitations obtained by exact diagonalization. Moreover, the present formalism nicely captures¹³ the charge order recently found by RXS¹¹. We therefore believe that the large- N theory is a powerful approach to explore charge excitations in cuprates.

III. RESULTS

In what follows we present results for the parameters $J/t = 0.3$ and $t'/t = 0.30$ which are appropriate for electron-doped cuprates¹³. The number of layers we take are 30, which is sufficiently large. We take $t_z = 0.1t$, for which we checked that the topology of the Fermi surface is the same as that for $t_z = 0$ in the doping region we will consider. Since that choice of t_z may be rather arbitrary, we will present the t_z dependence of our main results. Concerning the long-range Coulomb interaction [Eq. (2)], we choose $d/a = 1.5$ (Ref. 31) with $a = 4 \text{ \AA}$; while the choice of ϵ_{\parallel} and ϵ_{\perp} is not universal among theoretical papers^{25,32}, we respect the experimental data³³ and choose $\epsilon_{\parallel} = 4\epsilon_0$ and $\epsilon_{\perp} = 2\epsilon_0$ with ϵ_0 being the dielectric constant in vacuum. We present results mainly for $\delta = 0.15$, which allows us a direct comparison with recent experiments in the electron-doped cuprates^{14,15}.

We compute the spectral weight of the density-density correlation function $\text{Im}\chi^c(\mathbf{q}, \omega)$ after analytical continuation

$$i\omega_n \rightarrow \omega + i\Gamma \quad (14)$$

in Eq. (13). The value of Γ is positive and is in principle infinitesimally small. We choose $\Gamma = 10^{-4}t$ for numerical convenience in most of cases and will clarify the Γ dependence of our main results.

Figure 1 shows a map of the spectral weight $\text{Im}\chi^c(\mathbf{q}, \omega)$ in the plane of excitation energy ω and in-plane momentum \mathbf{q}_{\parallel} along symmetry axes of $(\pi, \pi) - (0, 0) - (\pi, 0) - (\pi, \pi)$. Below $\omega \sim 0.8t$, there is a particle-hole continuum coming from individual charge excitations. The continuum does not depend much on q_z except that the spectral weight is slightly enhanced along $(\pi, \pi) - (0, 0) - (\pi, 0)$ for $q_z = \pi$ compared with that for $q_z = 0$. In the figure the continuum for $q_z = 0$ is presented. We find no strong spectral weight near zero energy, implying that there is no charge order tendency associated with $\chi^c(\mathbf{q}, 0)$, namely the $(1, 1)$ component in the bosonic propagator of Eq. (4). Instead various charge orders can occur in the components specified by $a = b = 3, 4, 5$, and 6 as shown previously^{26,27}. In a high energy region, there is a sharp and strong weight for $q_z = 0$. This is a particle-hole bound state realized above the continuum, namely a plasmon. The plasmon energy at $\mathbf{q}_{\parallel} = (0, 0)$ is around $\omega_p = 0.7t$. Its dispersion is characterized by

$$\omega(\mathbf{q}_{\parallel}, q_z = 0) = \omega_p + a_2 q_{\parallel}^2 + \dots \quad (15)$$

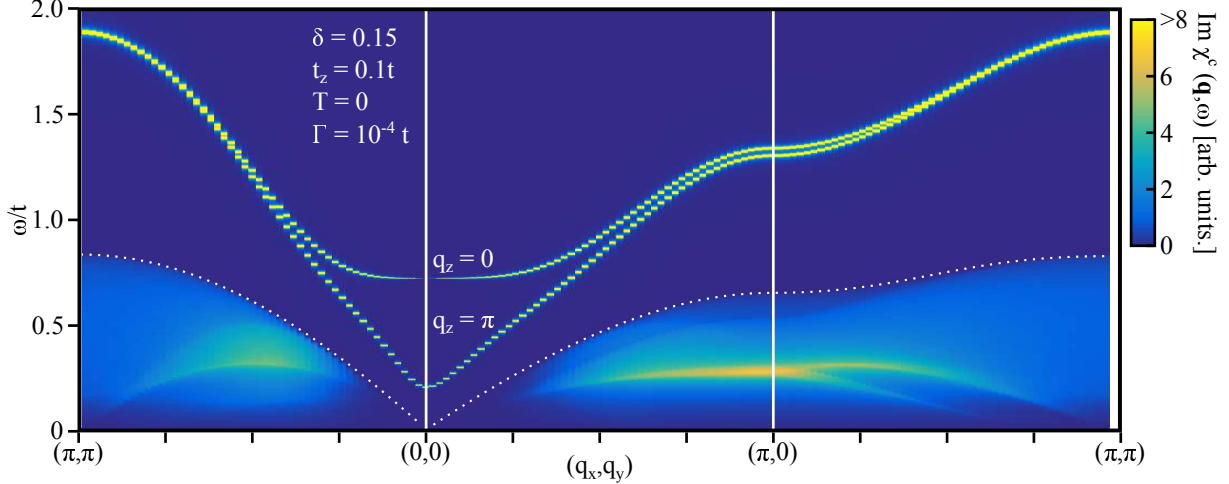


FIG. 1: (Color online) Spectral weight of the density-density correlation $\text{Im}\chi^c(\mathbf{q}, \omega)$ in the plane of energy ω and in-plane momentum \mathbf{q}_{\parallel} along $(\pi, \pi) - (0, 0) - (\pi, 0) - (\pi, \pi)$ for $q_z = 0$ and π . The dotted line denotes the upper boundary of a particle-hole continuum for $q_z = 0$. The spectral intensity of the plasmon is by far higher than the continuum and is cut at 8 to get a better contrast for the continuum.

The dispersion looks quite flat near $\mathbf{q}_{\parallel} = (0, 0)$, suggesting a very small value of a_2 . The coefficient of a_2 is approximated well by a formula obtained in the electron gas model³⁴, which predicts $a_2 = (3/10)v_F^2/\omega_p$ with v_F being the Fermi velocity; we may consider an average of the Fermi velocity in our case. Because the bare hopping integrals t , t' , and t_z are renormalized by a factor of $\delta/2$ in Eq. (7), our Fermi velocity becomes rather small at $\delta = 0.15$. This is a major reason why the plasmon dispersion is very flat near $\mathbf{q}_{\parallel} = (0, 0)$ in Fig. 1.

The plasmon dispersion changes drastically around $\mathbf{q}_{\parallel} = (0, 0)$ when q_z becomes finite. As a representative, we plot the plasmon dispersion for $q_z = \pi$ in Fig. 1. While the plasmon dispersion remains essentially the same as that for $q_z = 0$ far away from $\mathbf{q}_{\parallel} = (0, 0)$, the plasmon energy softens substantially near $\mathbf{q}_{\parallel} = (0, 0)$ and exhibits a strong dispersion there, in sharp contrast to that for $q_z = 0$. The plasmon has a quadratic dispersion near $\mathbf{q}_{\parallel} = (0, 0)$.

Figure 2 shows how the plasmon dispersion changes as increasing q_z from zero to π . Recalling that plasmons originate from the singularity of the long-range Coulomb interaction with $\sim 1/((\frac{\tilde{\epsilon}}{(a/d)^2}\mathbf{q}_{\parallel}^2 + q_z^2))$ [see Eq. (2)] at small momenta³⁴, the plasmon energy at $\mathbf{q}_{\parallel} = (0, 0)$ changes discontinuously once q_z becomes finite in a layered system. Because of this

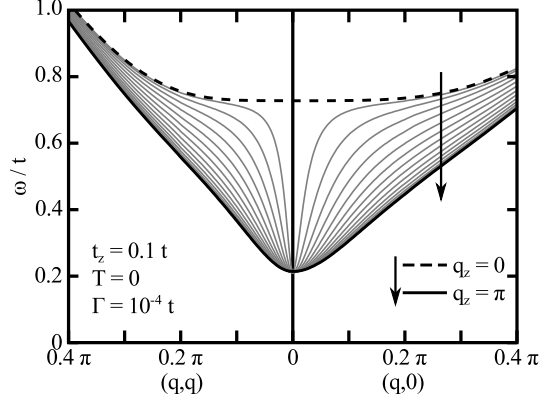


FIG. 2: q_z dependence of the plasmon dispersion around $\mathbf{q}_{\parallel} = (0, 0)$ along $(0.4\pi, 0.4\pi)$ - $(0, 0)$ - $(0.4\pi, 0)$. q_z is changed from zero to π with a step of $\pi/15$. This value of $\pi/15$ comes from our resolution of q_z since we take 30 layers in our model.

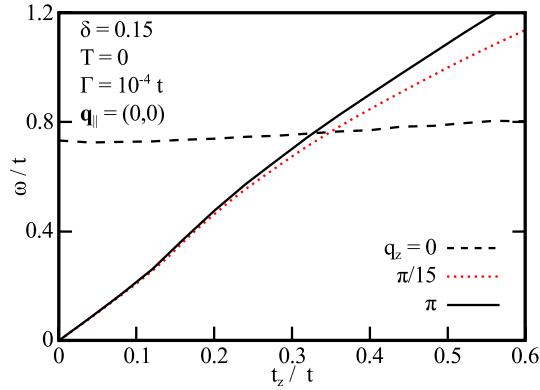


FIG. 3: (Color online) t_z dependence of the plasmon energy at $\mathbf{q}_{\parallel} = (0, 0)$ for $q_z = 0, \pi/15$, and π .

singularity, the plasmon dispersion becomes very sensitive to a slight change of q_z from zero for a small \mathbf{q}_{\parallel} . This strong q_z dependence of the plasmon mode was also obtained in literature^{19,20,22}, although $t_z = 0$ was assumed there.

In Fig. 3 we show the t_z dependence of the plasmon energy at $\mathbf{q}_{\parallel} = (0, 0)$ for several choices of q_z . At $q_z = 0$, the plasmon energy is almost independent of t_z . For a finite q_z , its t_z dependence becomes completely different from that for $q_z = 0$. As expected from Fig. 2, the plasmon energy at $\mathbf{q}_{\parallel} = (0, 0)$ drops discontinuously for a small t_z and exhibits almost the same t_z dependence for both $q_z = \pi/15$ and π . The plasmon energy vanishes at $t_z = 0$, in agreement with literature^{19,20,22}. As increasing t_z , the plasmon energy increases monotonically, with a linear dependence for a small t_z . Interestingly the plasmon energy

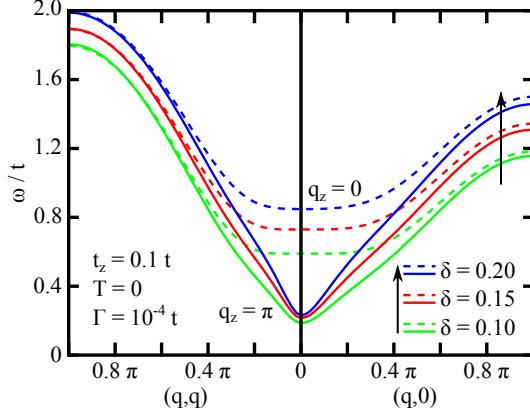


FIG. 4: (Color online) Plasmon dispersions for $q_z = 0$ (dashed line) and π (solid line) for several choices of doping rate δ along (π, π) - $(0, 0)$ - $(\pi, 0)$.

becomes higher than that at $q_z = 0$ for $t_z > 0.30t$ (see Appendix A). In Figs. 1 and 2 we take $t_z = 0.1t$ and thus the plasmon energy has $\omega \approx 0.2t$ at $\mathbf{q}_{\parallel} = (0, 0)$ for $q_z = \pi$ and $0.7t$ for $q_z = 0$.

The plasmon dispersions for $q_z = 0$ and π are summarized in Fig. 4 by performing calculations at different doping rates. The plasmon energy tends to increase with increasing doping. Since the plasmon energy at $\mathbf{q} = (0, 0, 0)$ is given by $\omega_p^2 = \frac{n_0 e^2}{\epsilon_0 m}$ in the electron gas model³⁴, where n_0 is the electron density and m is an electron mass, the hardening of the plasmon with carrier doping might be surprising since we would assume $n_0 = 1 - \delta$. However, electronic charge is introduced by carrier doping in the t - J model and there is no plasmon at half-filling³². We thus expect that the plasmon energy becomes higher with carrier doping at least close to half filling as shown in Fig. 4. See also Appendix B, where the plasmon energy is studied in the entire doping region $0 < \delta < 1$.

So far we have focused on calculations at temperature $T = 0$. Now we study the effect of temperature. In Fig. 5 (a) we plot $\text{Im}\chi^c(\mathbf{q}, \omega)$ at $\mathbf{q} = (0, 0, \pi)$ for several choices of temperatures. Surprisingly, not only the peak width but also the peak height is essentially unchanged with increasing $T (< 0.06t)$, although the peak position shifts slightly in a non-monotonic way: with raising temperature, the peak energy first increases a little bit and then decreases above $T \approx 0.025t$. This behavior reflects a weak temperature dependence of $\text{Re}\chi^c(\mathbf{q}, \omega)$ around $\omega \sim 0.2t$. If we invoke an unphysically large T , e.g., more than 500 K, which may correspond to $T > 0.05t$ if $t/2 = 500$ meV^{35,36}, the plasmon energy decreases and its peak height is gradually suppressed with further increasing T , keeping the peak width

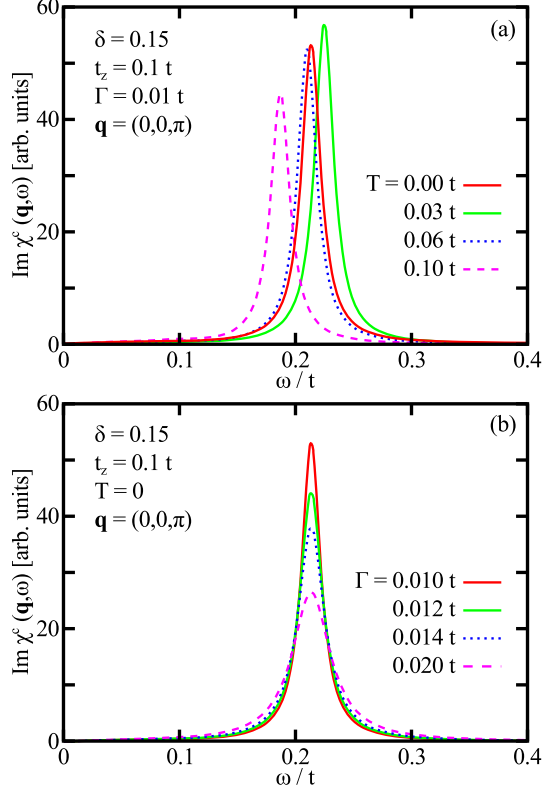


FIG. 5: (Color online) (a) Temperature dependence of $\text{Im}\chi^c(\mathbf{q}, \omega)$ at $\mathbf{q} = (0, 0, \pi)$ for $\Gamma = 0.01t$. (b) $\text{Im}\chi^c(\mathbf{q}, \omega)$ at $T = 0$ for several choices of Γ .

almost unchanged.

On the other hand, the peak height is quite sensitive to the damping factor Γ introduced in Eq. (14). Figure 5 (b) shows $\text{Im}\chi^c(\mathbf{q}, \omega)$ at $\mathbf{q} = (0, 0, \pi)$ at $T = 0$ for several choices of Γ . With increasing Γ the peak loses intensity and becomes slightly broader.

While we have taken Eq. (9) as the out-of-plane dispersion, we made the same calculations also for

$$\varepsilon_{\mathbf{k}}^{\perp} = 2t_z \frac{\delta}{2} \cos k_z \quad (16)$$

and found qualitatively the same results. We thus expect that our major results do not depend on details of the out-of-plane dispersion.

IV. DISCUSSIONS

We have studied plasmon modes, which are particle-hole bound states realized above the continuum (see Fig. 1), in a layered t - J model by including the long-range Coulomb interac-

tion. The plasmon dispersion is the usual optical mode at $q_z = 0$, but the dispersion changes drastically by shifting q_z slightly from zero (Fig. 2). The resulting dispersion becomes strong near $\mathbf{q}_{\parallel} = (0, 0)$ and its energy at $\mathbf{q}_{\parallel} = (0, 0)$ is scaled by t_z (Fig. 3).

Since the value of q_z is usually finite and well away from zero in RIXS, we consider that the mode observed by Lee *et al.*¹⁵ can be associated with the plasmon mode with a finite q_z , typically with $q_z = \pi$ (Figs. 1, 2, and 4). The gap magnitude at $\mathbf{q}_{\parallel} = (0, 0)$ obtained by the experiment¹⁵ is therefore interpreted to be proportional to the interlayer coupling t_z (Fig. 3). From a viewpoint of this plasmon scenario, it is interesting to clarify to what extent the present theory captures quantitative aspects. Our result suggests that $\omega \approx 2t_z$ for a small t_z in Fig. 3 and thus $t_z^{\text{exp}} \approx \frac{0.3\text{eV}}{2} = 0.15\text{ eV}$ as a bare hopping amplitude. Since the actual band width is renormalized by a factor of $\delta/2$ [see Eq. (9)], the obtained out-of-plane hopping at $(\pi, 0)$ becomes 90 meV. This value is a factor of three larger than the 30 meV obtained for single-layer cuprates (without apical oxygen atoms of Cu) by LDA²⁸. On the other hand, the slope of our plasmon dispersion near $\mathbf{q}_{\parallel} = (0, 0)$ for a finite q_z (Figs. 1, 2, and 4 for $q_z = \pi$) agrees with experimental observation within a factor of 1.5. In optical measurements¹⁶ and EELS^{17,18}, the value of q_z is zero. We thus expect naturally a large plasmon energy of the order of t . The q^2 dependence of the plasmon^{17,18} is nicely captured, but our coefficient a_2 [see Eq. (15)] is smaller than the experiments. In spite of these quantitative differences between the present theory and the experiments, our interpretation has the advantage to provide a consistent understanding of the mode recently found by Lee *et al.*¹⁵ and the mode observed by optical measurements¹⁶ and EELS^{17,18} by invoking a different value of q_z . This possibility was not considered by Lee *et al.*¹⁵.

The mode observed by Lee *et al.*¹⁵ exhibits a hardening with increasing carrier doping away from $\mathbf{q}_{\parallel} = (0, 0)$. This hardening is captured clearly in a large $|\mathbf{q}_{\parallel}|$ region for $q_z = \pi$ as shown in Fig. 4. In the vicinity of $\mathbf{q}_{\parallel} = (0, 0)$, on the other hand, Lee *et al.*¹⁵ reported a softening by comparing data at $x = 0.147$ and 0.166, which, however, looks quite subtle, whereas we have found a very small change even between $\delta = 0.15$ and 0.20. More comprehensive measurements for various dopings near $\mathbf{q}_{\parallel} = (0, 0)$ may be useful to make a further comparison. For $q_z = 0$, on the other hand, the hardening of the plasmon with increasing δ is consistent with experimental observation³⁷.

The temperature dependence of the charge excitation intensity obtained by Lee *et al.*¹⁵ could be understood within our framework. As shown in Fig. 5, the peak intensity of the

plasmon is rather delicate. Within a realistic range of temperature in Fig. 5 (a) ($< 0.05t$), not only the peak position but also the peak height and peak width do not change much. However, the peak height strongly depends on the damping factor Γ as shown in Fig. 5 (b). While Γ is introduced in the analytical continuation in Eq. (14), Γ may mimic a self-energy effect, especially for a relatively high energy region that we are interested in, because the imaginary part of the self-energy may not depend much on momentum and energy there. This feature allows us to consider the first term of the self-energy, namely a constant term, in Taylor series with respect to momentum and energy around the plasmon energy at $\mathbf{q} = (0, 0, \pi)$. If we invoke that Γ decreases with decreasing temperature, we may understand the temperature dependence of the charge excitation intensity at $\delta = 0.166$ observed by Lee *et al.*¹⁵. In contrast, the corresponding data at $\delta = 0.147$ in the experiment¹⁵ exhibits a much weaker temperature dependence, which can be due to a smaller temperature dependence of Γ in the corresponding temperature region.

In Ref. 14, a charge excitation peak near $\mathbf{q}_{\parallel} = (0, 0)$, which seems the same signal reported in Ref. 15, was interpreted in terms of individual particle-hole excitations, not a collective mode such as the plasmon. If the individual excitations are responsible for that, one would expect a gapless excitation spectrum at $\mathbf{q}_{\parallel} = (0, 0)$. It is therefore worth performing RIXS measurements more in detail near $\mathbf{q}_{\parallel} = (0, 0)$ to clarify whether the gap is indeed present at $\mathbf{q}_{\parallel} = (0, 0)$ or not, which is a crucial test of our interpretation of plasmons.

As frequently seen in standard textbooks in condensed matter physics³⁴, a plasmon mode is often presumed to overdamp as momentum transfer becomes large because of the mixture with the particle-hole continuum. Such a result is obtained in an electron gas in a continuum model. On the other hand, in a layered system defined on a lattice, which is more realistic to cuprates, we find that the plasmon is well separated from the particle-hole continuum up to the zone boundary (see Fig. 1). It is, however, noted that the present one-band model contains only intraband scattering processes and in general there should be also various interband scattering processes in real materials. The plasmon is thus likely overdamped due to the mixture of the interband excitations. At present, available data¹⁴ suggest that the interband spectral weight is dominant only rather close to $\mathbf{q}_{\parallel} = (0, 0)$ around $\omega = 2\text{ eV}$. Hence it is interesting to test how the mode observed by Lee *et al.*¹⁵ disperses for a large $|\mathbf{q}_{\parallel}|$.

The two experimental works, Refs. 14 and 15, should not be mixed with Ref. 11. For the

former studies (Refs. 14 and 15), we here propose plasmon modes to interpret the charge-excitation peak observed around $\mathbf{q}_{\parallel} = (0, 0)$ in a relatively high energy region. For the latter (Ref. 11), the charge order signal was observed at $\mathbf{q}_{\parallel} \approx (0.48\pi, 0)$, far away from $\mathbf{q}_{\parallel} = (0, 0)$. This data can be interpreted in terms of d -wave bond-order charge excitations described by the third and fourth components of D_{ab} in Eq. (4), as shown in our previous work¹³. While the long-range Coulomb interaction was not considered previously¹³, its impact on the d -wave bond-order is expected to be very weak since the D_{11} and D_{ab} with $a, b = 3, 4$ are almost decoupled with each other^{26,27}.

The present study can be highlighted also through a comparison with previous theoretical studies of plasmons in cuprates. First, we share a strong q_z dependence of the plasmon dispersion with early theoretical studies^{19,20,22}. Second, previous calculations^{19–22} did not take the interlayer hopping t_z into account and reported a gapless dispersion for a finite q_z . However, we have shown a striking insight that the plasmon mode has a sizable gap with a quadratic dispersion near $\mathbf{q}_{\parallel} = (0, 0)$ for a finite q_z because of a finite interlayer hopping t_z . This aspect is very important to study charge excitations in cuprates. Third, Ref. 22 predicts that the plasmon for $q_z = 0$ has a very steep dispersion around $\mathbf{q}_{\parallel} = (0, 0)$ whereas we have obtained a very flat dispersion (Figs. 1 and 4 for $q_z = 0$). Fourth, previous studies^{19,20,22} are based on a weak coupling theory and consider the presence of the long-range Coulomb interaction even at half-filling, whereas, consistent with a phenomenology of a Mott insulator²¹, the long-range Coulomb interaction vanishes at half-filling in the present large- N theory.

Our obtained results (Fig. 1) are expected to be a representative of cuprate superconductors in general. Although a mode similar to that observed by Lee *et al.*¹⁵ has not been reported yet in hole-doped cuprates, we expect that a similar mode should be present and can be detected by RIXS at least in a normal state in a heavily doped region where the pseudogap effect is substantially weakened. A recent RIXS study by Ishii *et al.*³⁸ suggests the presence of charge excitations near $\mathbf{q}_{\parallel} = (0, 0)$ in $\text{La}_{2-x}\text{Sr}_x\text{CuO}_4$ similar to that observed in NCCO^{14,15}.

V. CONCLUSIONS

In summary, we have studied plasmon excitations in the t - J model by including an interlayer coupling and the long-range Coulomb interaction as a generic model of the layered cuprate superconductors. We have found that the plasmon dispersion exhibits a strong q_z dependence in the vicinity of $\mathbf{q}_{\parallel} = (0, 0)$ (Figs. 1 and 2). For $q_z = 0$ the plasmon has a large energy gap of the order of t near $\mathbf{q}_{\parallel} = (0, 0)$, which may be associated with the mode observed in optics¹⁶ and EELS^{17,18}. For a finite q_z , on the other hand, the plasmon energy is substantially suppressed to a low energy at $\mathbf{q}_{\parallel} = (0, 0)$ and exhibits a strong dispersive feature (see Figs. 1, 2, and 4). We have also found that the plasmon energy at $\mathbf{q}_{\parallel} = (0, 0)$ for a finite q_z is scaled by the interlayer hopping amplitude t_z (Fig. 3). Since q_z is in general finite in RIXS measurements, the mode observed by Lee *et al.*¹⁵ can be associated with the plasmon mode with a finite q_z . The present results should not be mixed with a recent observation of a short-range charge order by RIXS¹¹. Within essentially the same large- N framework as the present one, that charge-order peak was interpreted in terms of the d -wave bond-order correlation function¹³, which has a dominant spectral weight far away from $\mathbf{q}_{\parallel} = (0, 0)$ and in energy much lower than the plasmon. While we have presented results for a parameter set appropriate for electron-doped cuprates, our results are expected to be applicable to hole-doped cuprates at least in the normal state in the overdoped side where the effect of the pseudogap is substantially weakened, implying that the plasmon mode will be observed by RIXS also in hole-doped cuprates.

Acknowledgments

The authors thank K. Ishii for very fruitful discussions about RIXS measurements in cuprates. H.Y. acknowledges support by a Grant-in-Aid for Scientific Research Grant No. JP15K05189.

Appendix A: Plasmons for a large t_z

While a realistic value of t_z in cuprates is expected much smaller than t in Fig. 3, it is interesting that the plasmon energy for $q_z = \pi$ becomes larger than that for $q_z = 0$ for a large t_z . This is demonstrated in Fig. 6 by computing plasmon dispersions for $t_z =$

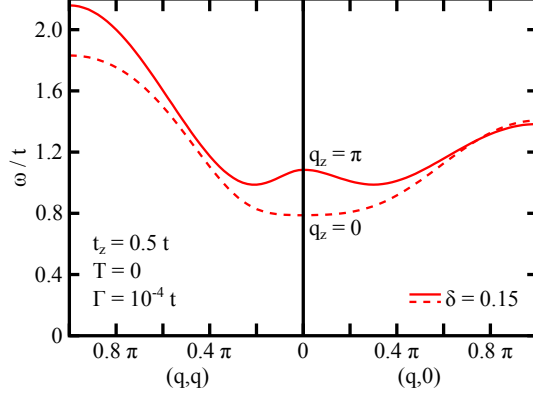


FIG. 6: (Color online) Plasmon dispersions for $q_z = 0$ (dashed line) and π (solid line) for $\delta = 0.15$ and $t_z = 0.5t$ along (π, π) - $(0,0)$ - $(\pi, 0)$.

$0.5t$ as a function of \mathbf{q}_{\parallel} , which may be applicable to a layered material with strong three dimensionality. Interestingly, the dispersion for $q_z = \pi$ has a negative curvature at $\mathbf{q}_{\parallel} = (0, 0)$ and forms local minima at $\mathbf{q}_{\parallel} \approx (0.3\pi, 0)$ and $(0.2\pi, 0.2\pi)$. For a larger $|\mathbf{q}_{\parallel}|$, the dispersion for $q_z = \pi$ shows a dependence similar to that for $q_z = 0$.

Appendix B: Doping dependence of plasmon energy

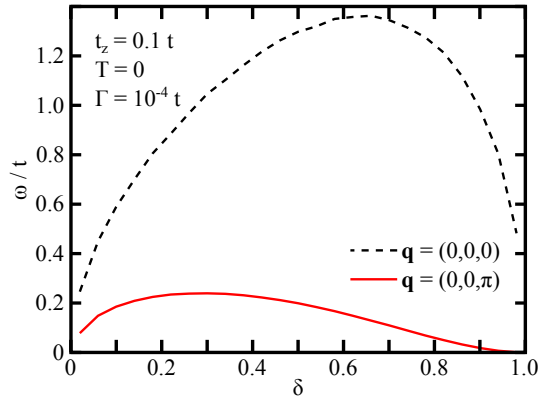


FIG. 7: (Color online) Plasmon energy at $\mathbf{q} = (0, 0, 0)$ (dashed line) and $(0, 0, \pi)$ (solid line) as a function of doping.

In Fig. 4, we have presented the plasmon dispersions for several choices of δ . Figure 7 is a complementary result by plotting the plasmon energy at $\mathbf{q}_{\parallel} = (0, 0)$ as a function of δ . The plasmon energy for both $q_z = 0$ and π increases with δ at least in a doping region

realistic to cuprates ($\delta \lesssim 0.30$). This is consistent with a previous work in the t - J model³², where the plasmon energy for $q_z = 0$ was studied as a function of δ . The plasmon energy forms a maximum and then decreases for a high δ . This is easily understood by noting that the electronic band becomes empty at $\delta = 1$, where the plasmon energy would vanish.

-
- ¹ G. Ghiringhelli, M. Le Tacon, M. Minola, S. Blanco-Canosa, C. Mazzoli, N. B. Brookes, G. M. D. Luca, A. Frano, D. G. Hawthorn, F. He, et al., *Science* **337**, 821 (2012).
- ² J. Chang, E. Blackburn, A. T. Holmes, N. B. Christensen, J. Larsen, J. Mesot, R. Liang, D. A. Bonn, W. N. Hardy, A. Watenphul, et al., *Nat. Phys.* **8**, 871 (2012).
- ³ A. J. Achkar, R. Sutarto, X. Mao, F. He, A. Frano, S. Blanco-Canosa, M. Le Tacon, G. Ghiringhelli, L. Braicovich, M. Minola, et al., *Phys. Rev. Lett.* **109**, 167001 (2012).
- ⁴ E. Blackburn, J. Chang, M. Hücker, A. T. Holmes, N. B. Christensen, R. Liang, D. A. Bonn, W. N. Hardy, U. Rütt, O. Gutowski, et al., *Phys. Rev. Lett.* **110**, 137004 (2013).
- ⁵ S. Blanco-Canosa, A. Frano, E. Schierle, J. Porras, T. Loew, M. Minola, M. Bluschke, E. Weschke, B. Keimer, and M. Le Tacon, *Phys. Rev. B* **90**, 054513 (2014).
- ⁶ R. Comin, A. Frano, M. M. Yee, Y. Yoshida, H. Eisaki, E. Schierle, E. Weschke, R. Sutarto, F. He, A. Soumyanarayanan, et al., *Science* **343**, 390 (2014).
- ⁷ E. H. da Silva Neto, P. Aynajian, A. Frano, R. Comin, E. Schierle, E. Weschke, A. Gyenis, J. Wen, J. Schneeloch, Z. Xu, et al., *Science* **343**, 393 (2014).
- ⁸ M. Hashimoto, G. Ghiringhelli, W.-S. Lee, G. Dellea, A. Amorese, C. Mazzoli, K. Kummer, N. B. Brookes, B. Moritz, Y. Yoshida, et al., *Phys. Rev. B* **89**, 220511 (2014).
- ⁹ W. Tabis, Y. Li, M. Le Tacon, L. Braicovich, A. Kreyssig, M. Minola, G. Dellea, E. Weschke, M. J. Veit, M. Ramazanoglu, et al., *Nat. Commun.* **5**, 5875 (2014).
- ¹⁰ S. A. Kivelson, I. P. Bindloss, E. Fradkin, V. Oganesyan, J. M. Tranquada, A. Kapitulnik, and C. Howald, *Rev. Mod. Phys.* **75**, 1201 (2003).
- ¹¹ E. H. da Silva Neto, R. Comin, F. He, R. Sutarto, Y. Jiang, R. L. Greene, G. A. Sawatzky, and A. Damascelli, *Science* **347**, 282 (2015).
- ¹² A pseudogap was reported in a state above the antiferromagnetic state in electron-doped cuprates³⁹, but the pseudogap similar to the hole-doped case, i.e., a gap-like feature above the onset temperature of superconducting instability is missing or at least very weak.

- ¹³ H. Yamase, M. Bejas, and A. Greco, *Europhys. Lett.* **111**, 57005 (2015).
- ¹⁴ K. Ishii, M. Fujita, T. Sasaki, M. Minola, G. Dellea, C. Mazzoli, K. Kummer, G. Ghiringhelli, L. Braicovich, T. Tohyama, et al., *Nat. Commun.* **5**, 3714 (2014).
- ¹⁵ W. S. Lee, J. J. Lee, E. A. Nowadnick, S. Gerber, W. Tabis, S. W. Huang, V. N. Strocov, E. M. Motoyama, G. Yu, B. Moritz, et al., *Nat. Phys.* **10**, 883 (2014).
- ¹⁶ E. J. Singley, D. N. Basov, K. Kurahashi, T. Uefuji, and K. Yamada, *Phys. Rev. B* **64**, 224503 (2001).
- ¹⁷ N. Nücker, H. Romberg, S. Nakai, B. Scheerer, J. Fink, Y. F. Yan, and Z. X. Zhao, *Phys. Rev. B* **39**, 12 379 (1989).
- ¹⁸ H. Romberg, N. Nücker, J. Fink, T. Wolf, X. X. Xi, B. Koch, H. P. Geserich, M. Dürmler, W. Assmus, and B. Gegenheimer, *Z. Phys. B* **78**, 367 (1990).
- ¹⁹ V. Z. Kresin and H. Morawitz, *Phys. Rev. B* **37**, 7854 (1988).
- ²⁰ A. Bill, H. Morawitz, and V. Z. Kresin, *Phys. Rev. B* **68**, 144519 (2003).
- ²¹ E. G. C. P. van Loon, H. Hafermann, A. I. Lichtenstein, A. N. Rubtsov, and M. I. Katsnelson, *Phys. Rev. Lett.* **113**, 246407 (2014).
- ²² R. S. Markiewicz, M. Z. Hasan, and A. Bansil, *Phys. Rev. B* **77**, 094518 (2008).
- ²³ A. Foussats and A. Greco, *Phys. Rev. B* **70**, 205123 (2004).
- ²⁴ T. Thio, T. R. Thurston, N. W. Preyer, P. J. Picone, M. A. Kastner, H. P. Jenssen, D. R. Gabbe, C. Y. Chen, R. J. Birgeneau, and A. Aharony, *Phys. Rev. B* **38**, 905 (1988).
- ²⁵ F. Becca, M. Tarquini, M. Grilli, and C. Di Castro, *Phys. Rev. B* **54**, 12443 (1996).
- ²⁶ M. Bejas, A. Greco, and H. Yamase, *Phys. Rev. B* **86**, 224509 (2012).
- ²⁷ M. Bejas, A. Greco, and H. Yamase, *New J. Phys.* **16**, 123002 (2014).
- ²⁸ O. K. Andersen, A. I. Lichtenstein, O. Jepsen, and F. Paulsen, *J. Phys. Chem. Solids* **56**, 1573 (1995).
- ²⁹ A. T. Hoang and P. Thalmeier, *J. Phys.: Condens. Matter* **14**, 6639 (2002).
- ³⁰ J. Merino, A. Greco, R. H. McKenzie, and M. Calandra, *Phys. Rev. B* **68**, 245121 (2003).
- ³¹ Although CuO_2 planes shift by $(\frac{1}{2}, \frac{1}{2}, \frac{1}{2})$ in NCCO, we model the actual system by neglecting such a shift for simplicity. Our interlayer distance d is thus given by a half of the c -axis lattice constant.
- ³² P. Prelovšek and P. Horsch, *Phys. Rev. B* **60**, R3735 (1999).
- ³³ T. Timusk and D. Tanner, *Infrared properties of high- T_c superconductors* (Word Scientific,

Singapore, 1989).

- ³⁴ G. D. Mahan, *Many-Particle Physics* (Plenum, New York, 1990), 2nd ed.
- ³⁵ M. S. Hybertsen, E. B. Stechel, M. Schluter, and D. R. Jennison, *Phys. Rev. B* **41**, 11068 (1990).
- ³⁶ A factor of $1/2$ here comes from a large- N formalism where t is scaled by $1/N$. We may assume $N = 2$ in comparison with experiments.
- ³⁷ J. Hwang, T. Timusk, and G. Gu, *J. Phys.: Condens. Matter* **19**, 125208 (2007).
- ³⁸ K. Ishii (private communication).
- ³⁹ Y. Onose and Y. Taguchi and K. Ishizaka and Y. Tokura, *Phys. Rev. Lett.* **87**, 217001 (2001).